World Journal of Advanced Research and Reviews
eISSN: 2581-9615 CODEN (USA): WJARAI
Cross Ref DOI: 10.30574/wjarr
Journal homepage: https://wjarr.com/

(RESEARCH ARTICLE)

Check for updates

Study of the structural, electronic, optical, and elastic properties of $NaSrAt_3$ perovskites using density functional theory (DFT) with GGA formalism

Mona Hermann Charly YAPI [1, 2, *], Koffi Charles Kouman [2], Mélèdje C. Désiré [2, 3], Guy Müller Banquet OKRA [1, 2], Womblegnon Stephane GUIA [1] and Kré N. Raymond [2]

[1] *Laboratory of Environmental Sciences and Technologies (LSTE), University JEAN LOROUGNON GUÉDÉ (UJLoG), Daloa, BP 150 Daloa, Côte d'Ivoire.*
[2] *Laboratory of Fundamental and Applied Physics (LPFA), University NANGUI ABROGOUA (UNA), Abidjan, BP 801 Abidjan 02, Côte d'Ivoire.*
[3] *Institute for Research on New Energies (IREN), University NANGUI ABROGOUA (UNA), Abidjan, BP 801 Abidjan 02, Côte d'Ivoire.*

World Journal of Advanced Research and Reviews, 2025, 28(01), 1929-1941

Publication history: Received on 19 September 2025; revised on 25 October 2025; accepted on 27 October 2025

Article DOI: https://doi.org/10.30574/wjarr.2025.28.1.3654

Abstract

The structural, electronic, optical and elastic properties of the $NaSrAt_3$ perovskite were studied through Density Functional Theory (DFT) using the GGA formalism. $NaSrAt_3$ has for lattice parameters obtained are 5.15 Å. The gap energy is 0.762 eV and is indirect on the Γ-R path of the Brillouin zone. The valence band is characterized by the 1s state of At and the conduction band by the 4p state of Na, 2s of Sr and 4p of Sr. The charge density shows a probable bond between atoms Na and At and between atoms Sr and At. Light passing through the material is likely to be slower to propagate and be deflected in IR and visible. From 2 eV to 10 eV, $NaSrAt_3$ has a real refractive index $n(\omega)$ practically zero and the optical conductivity $\sigma(\omega)$ is high from 0 eV to 4 eV and low from 4 eV to 10 eV indicating that electron transport occurs from 0 eV to 4 eV. The studied elastic properties show that NaSrAt3 has a high fragility but stable. It has an isotropic character and low and slightly rigid hardness. It has ionic bonds. The resulting melting temperature is high. As many properties to affirm that NaSrAt3 can be used in photovoltaic cells and other electronic devices.

Keywords: Perovskites NaSrAt3; DFT; Electronic; optical; Elastic properties

1. Introduction

The energy resources that have long been the basis of humanity's economic development are constantly declining, depleting day by day. Exploiting them becomes a journey too calamitous for the environment. What to do in the face of this great disaster so predictable? However, we must not have as a drastic solution to additionally stop the so large energy consumption that our current civilization needs. The best solution would be to replace these conventional energy sources with cleaner, environmentally friendly and inexhaustible other energy sources. And what other best candidate can he have than renewable energies? the advantage of renewable energies is their abundance on the planet. In addition to that, exploitation does not influence the environment in any way. Their accessibility is so legendary that they could provide any solution to global energy needs again and again. Humanity would benefit more from investing in these renewable energies. They are numerous, but one is very promising: photovoltaic energy. For a few years, research has been constantly done on solar cells. Several materials are used in this direction as an active layer. Silicon is the most used. Many other materials exist such as thin films, cadmium telluride (CdTe), copper-indium-gallium selenide (CIGS), hybrids, multi-junctions, tandems ... All these cells have an appreciable efficiency, like the multi-cell solar cellsjunctions made up of several thin films deposited by organometallic vapor phase epitaxy or by molecular

* Corresponding author: Mona Hermann Charly YAPI

beam epitaxy which reaches a record photovoltaic conversion efficiency of 47.1% [1]. However, all these cells pose the same drawbacks as silicon cells: a high production cost and the use of basic materials harmful to the environment. To make photovoltaic energy a likely candidate for energy alternation, it is necessary to turn towards other materials that are more accessible and operating without harming the environment and which will make the cost of producing cells more affordable. The materials that will undoubtedly do the job are perovskites. These decades, some studies on perovskite solar cells have achieved an efficiency of 20% in 2015, compared to the efficiency of silicon-based cells which is 25% [2,3]. Solar cells have several advantages: good absorption of the solar spectrum, good flexibility and lightness, low-temperature manufacturing; which reduce the production cost. These materials are also very abundant on our planet. However, the perovskites with a good yield are organic perovskites. Now, organic perovskites are known to have stability problems. This problem could be addressed by using inorganic perovskites known to be much more stable than their organic counterparts. It should be noted, however, that inorganic perovskite cells have a low conversion efficiency compared to inorganic perovskite cells [4]. To increase their yields, research will need to be conducted on these materials. This is the reason why, in our work, we studied the structural, electronic, optical and elastic properties of the NaSrAt3 perovskite by Density Functional Theory (DFT) using the GGA formalism.

2. Materials and Methods

2.1. Materials

We made use of the software suite Quantum Expresso (qe-7.0) [5,6,7] which integrates several other sub-programs each performing a specific task. The computing resource used is a 2.90 GHz frequency core i7 computer (Lenovo series). Other programs have also been used to process the data generated by Quantum-espresso. One can name Vesta, Gnu plot, and Grace. The study material is the $NaSrAt_3$ perovskite structure of cubic crystalline structure Pm3m. It contains five atoms in its crystalline mesh. Figure 1 shows a representation of the crystal structure.

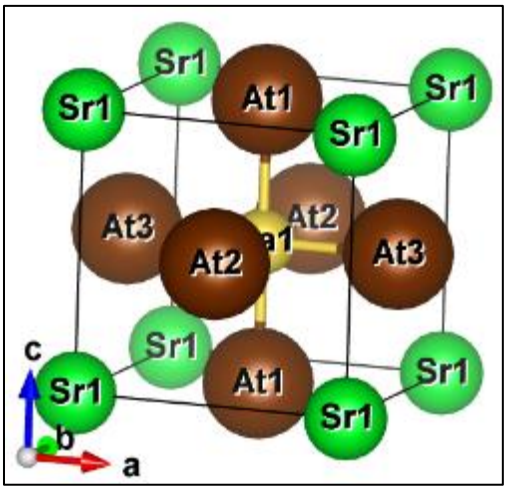

Figure 1 Cubic crystal structure of $NaSrAt_3$

2.2. Method

The method used in this work is the quantum calculation method of density functional theory (DFT). The DFT integrates several formalisms. In this study, we used is the generalized gradient approximation (GGA) of Perdew, Burke and Ernzerhof (PBE + GGA) [8,9,10]. The calculation needs a fairly high level of convergence. We have therefore set the convergence level to 10-9 (1.0d-9 eV). We chose to divide into 12×12×12 for the number of mesh points k in the Brillouin area. The kinetic energy of cut-off (ecut) is a very important factor for such a DFT calculation. We have therefore chosen to set ours to 80 Ry. All the parameters were obtained by a structural relaxation calculation. DFT is implemented by the Quantum Espresso code [5,6].

3. Results and discussion

3.1. Convergence test

A DFT calculation is indeed executed if the parameters used in the calculation have been relaxed. A convergence test of each quantity is therefore necessary. This convergence test will lead to optimal values of the equilibrium structural quantities of the perovskite $NaSrAt_3$ to be studied. These optimized parameters are: the mesh parameter, the kinetic energy of cut-off, the k-points of Monkhorst-Pack in the Brillouin zone. This convergence test is done by vc_relax calculation taking place in iterations. This leads to a value corresponding to the smallest energy of the system. The most stable system is what corresponds to this stable value of the parameter.

3.1.1. Lattice parameter

We present in figure 2, the evolution of the total energy of the system as a function of the evolution of the cell parameter of the perovskite material NaSrAt3. At the smallest energy value corresponds the equilibrium cell parameter.

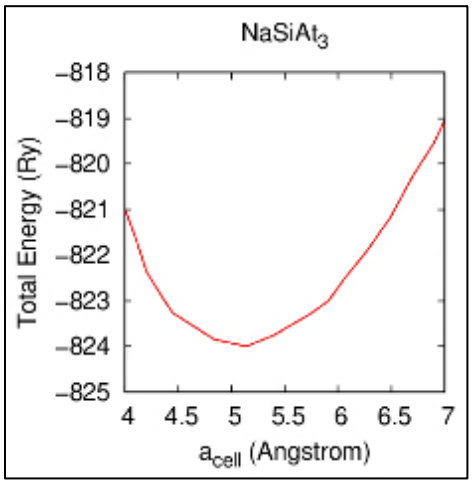

Figure 2 Convergence of Lattice Parameter acell of $NaSrAt_3$ perovskite

Table 1 shows the calculated cell parameter of $NaSrAt_3$. The cell parameter obtained is 5.15 Å. Compared to other authors such as M T Hossain et al [11,12] who studied the compounds $XSrBr_3$(X = Na, Ga, and Tl) and AXI_3(A = Li, Na; X = Ca, Sr, Ba), our cell parameter is lower.

Table 1 Lattice Parameter a cell of NaSrAt3 perovskite

Latice parameter a_{cell} in Å		
Materials	Our results	Literature results
$NaSrAt_3$	5.15	-

3.1.2. Convergence of Kinetic energy cut-off

Kinetic cutoff energy indicates the cutoff of the number of plane wave functions used as basis functions to represent the wave function. In theory, an infinite number of basis functions are required to obtain an exact answer. Which is almost impossible. To circumvent this difficulty, it is therefore necessary to introduce the kinetic energy of cut-off (ecut). It represents the kinetic energy of the wave function of electrons in the crystal that the latter cannot reach [5,6,13]. Figure 3 presents the evolution of total energy with kinetic energy of cut-off. The vc_relax calculation gives an ecut of 70 Ry. The calculation will be precise if the kinetic energy of cut-off is high, however the computer resource will be important, the calculation time too. We have therefore chosen to set the kinetic energy of cut-off at 80 Ry.

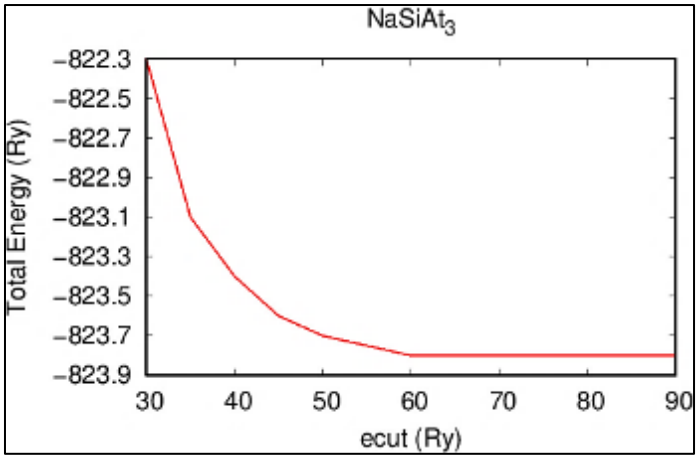

Figure 3 Convergence of Kinetic energy cut-off ecut of $NaSrAt_3$ perovskite

3.1.3. Convergence of k-point

We used the Monkhorst-Pack method [13] to sample the k points of the Brillouin zone. The relaxation gives a convergence of 6×6×6 of point k. However, for more precision in this work, we have chosen 12×12×12 for meshing. This precision is good because it is known that for very good precision, a k-point mesh of at least 8×8×8.

3.2. Electronic properties

In this paragraph, we elaborate the different electronic properties obtained from $NaSrAt_3$ perovskite materials. These electronic properties are: band structure, total density (TDOS), partial state densities (PDOS) and charge density.

3.2.1. Bands structure

The electronic band structure provides a description of the energy levels allowed to electrons in the solid. These energy levels result from the interaction between atoms in the solid. This interaction forms continuous bands instead of discrete levels. Two interesting bands emerge then: the valence band (occupied) and the conduction band (empty). These two bands are separated by the band gap. The structure of bands allows to describe the magnetic, electronic, optical and thermal properties of a material [15]. Figure 4 shows the electronic band structure of the perovskite $NaSrAt_3$ according to the direction of the high symmetry points X-R-M-X-R-M-Γ-X of the first Brillouin zone. Using the electronic structure of bands, we obtain the gap. The gap is the difference between the bottom of the condition band and the top of the valence band. The width of the gap is indicative of the type of material. Between these two bands lies the fermi level. We can also see the type of gap: direct or indirect. It is insulating if the gap is greater than 5 eV and semiconductor if the gap is less than eV [16]. In the case of a conductor, valence band and conduction band overlap: the gap is zero.

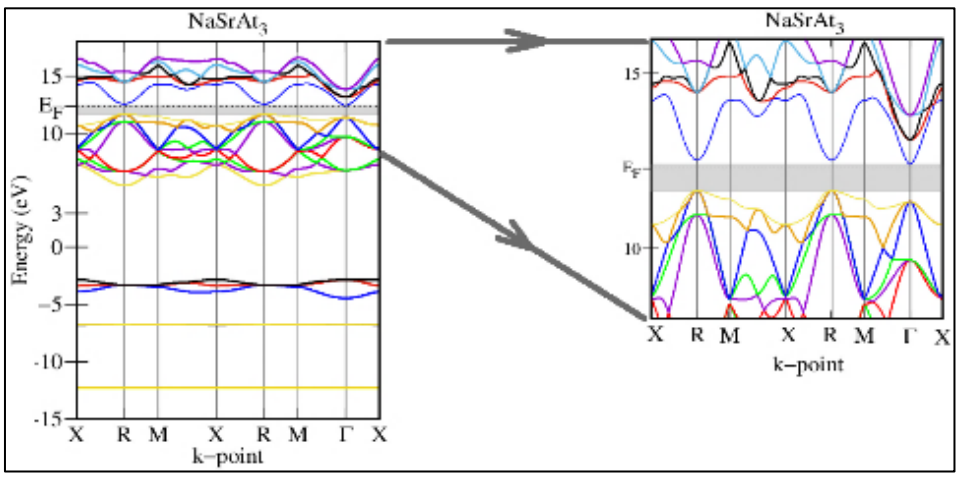

Figure 4 Electronic band structure of $NaSrAt_3$

Table 2 presents the resulting gap. We obtain a gap of 0.762 eV. $NaSrAt_3$ is therefore semiconductor. This gap is low, compared to $NaSrBr_3$ and $NaSrI_3$ for which M T Hossain et al [10, 11] obtained a gap of 2.95 and 2.41 eV respectively and M H C Yapi et al [17] 2.51 eV and 1.49 eV, respectively. There is no work done in the literature for the $NaSrAt_3$ perovskite. We therefore compare our results to other perovskites of the same type in the literature. $NaSrAt_3$ has an indirect gap in the Γ-R direction. This offers rather electronic applications.

Table 2 Gap values and energy gap at high symmetry points for perovskite $NaSrAt_3$.

$NaSrAt_3$ perovskite			
	Our results		Literature results
Gap (eV)	0.762		-
Type of gap	Indirect Γ-R		-
Fermi level	12.292 eV		-
Energy gap at high symmetry points	R-R	0.878	-
	M-M	3.821	-
	X-X	3.554	-
	Γ-Γ	1.054	-
	M-Γ	3.009	-
	R-X	2.675	-
	R-M	2.670	-
	R- Γ	0.974	-
	X-M	3.549	-

3.2.2. Partial and total densities of state

To understand the contribution of the different atomic orbitals and the nature of the bonds between atoms in the material, it is necessary to study the total state density (TDOS) and the partial state densities (PDOS). Figure 5 shows the total state density (TDOS) and partial state densities (PDOS) of the $NaSrAt_3$ perovskite. The valence band of $NaSrAt_3$ is characterized by the very dominant 1s-At state in the valence band. The 1s -At state is weakly mixed with the 2s-Sr and 4p-Na states.

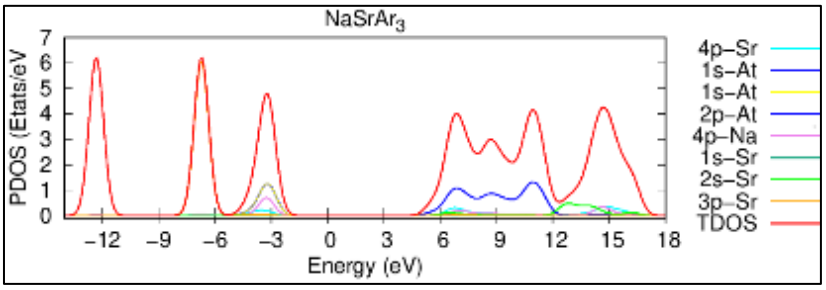

Figure 5 Calculated total and partial densities of states for $NaSrAt_3$

The conduction band is characterized by the 4p-Na, 2s- Sr and 4p- Sr state. Upon observing the TDOS of the PDOS, it is noted that the valence band and the conduction band are completely confused. In fact, the state 2s- Sr makes the junction between these two bands. This makes $NaSrAt_3$ almost conductive. With figure 6, the different borders around the gap are represented.

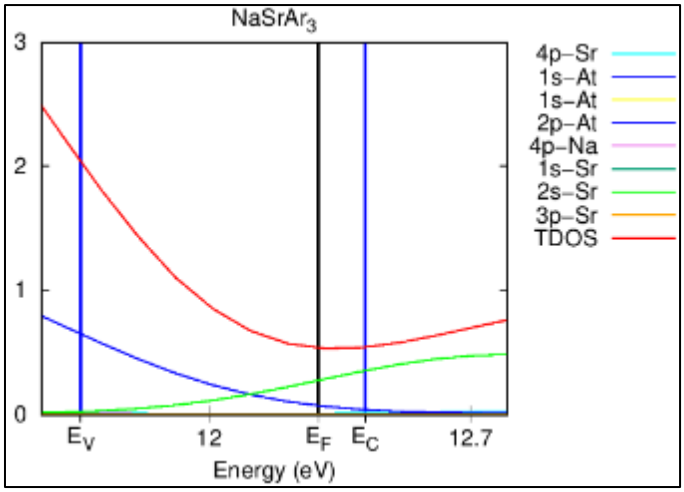

Figure 6 Observation of the edges of bands of calculated state densities for $NaSrAt_3$

The states 1s- At and 2s-Sr exceed the band gap; they almost overlap in the gap. We can therefore conclude that the 1s-At and 2s- Sr states restore a very significant character for the $NaSrAt_3$ material in the sense that it ensures an almost conductive character to this material. The fermi level seems much closer to the conduction band. To understand the binding behavior and how charges are distributed between atoms of the material, it is necessary to observe the charge density of $NaSrAt_3$. It is presented in the crystallographic directions (110) by figure 7 and (100) by figure 8.

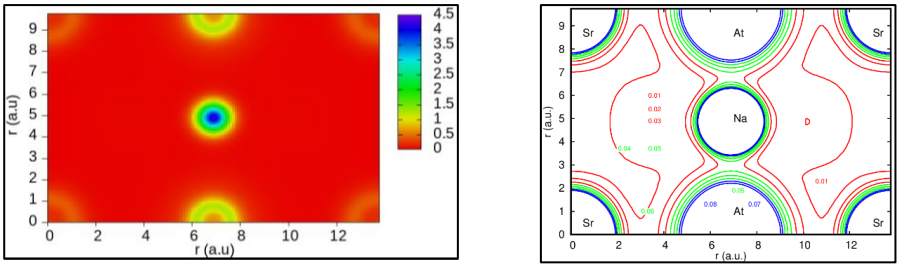

Figure 7 Charge density of $NaSrAt_3$ in crystallographic plane (110)

The type of bond that exists between atoms is provided by the charge density graph of the material [18]. Thus, in the crystallographic plane (110), one can see that a strong interaction exists between neighboring atoms Na and At. There is therefore hybridization between these atoms. This suggests a Na-At covalent bond in the perovskite and charge transfer between Na and At. It was the same observation for $NaSrX_3$(x=F, Cl, Br and I) studied by Yapi et al [17]. In the crystallographic plane (100) (figure 8), there is an interaction between atoms Ar and its neighbors Sr, however less strong than that observed in the crystallographic plane (110). We assume that a covalent bond Sr-At in this perovskite. There is the transfer of charges between Sr and At. This latter observation is quite different from that of the $NaSrX_3$ compounds (x=F, Cl, Br and I) studied by Yapi et al [17].

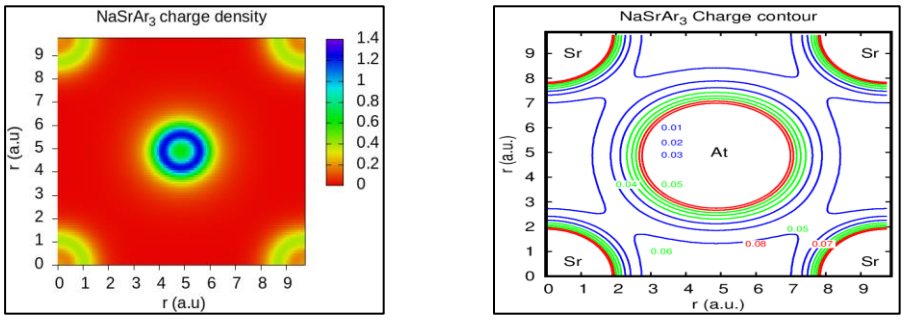

Figure 8 Charge density of $NaSrAt_3$ in crystallographic plane (100)

3.3. Optical properties

3.3.1. Real part and imaginary part of the complex dielectric function

The description of the optical properties of a material is done through a study of the complex dielectric function $\tilde{\varepsilon}$. The complex dielectric function describes the reaction of the material in front of light. Indeed, when light falls on the material, the response of this material is described by the complex dielectric function $\tilde{\varepsilon}$. It is written: $\tilde{\varepsilon}(\omega) = \varepsilon_r(\omega) + i\varepsilon_i(\omega)$. ε_r is the real part and ε_i, the imaginary part. The other optical functions are deduced from it. The complex dielectric function of $NaSrAt_3$ are represented by figure 9.

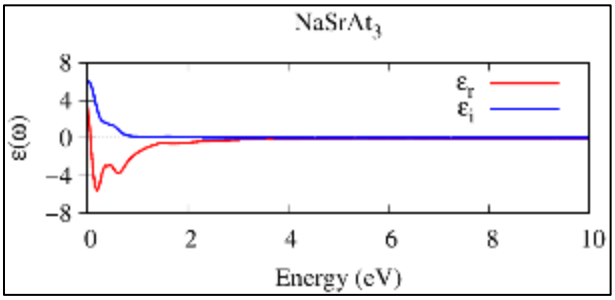

Figure 9 Real part (in red) and imaginary part (in blue) of the dielectric function calculated

Two parts emerge: from 0 to 4 eV and from 4 to 10 eV. From 0 to 4 eV, the two curves show some fluctuations. From 4 to 10 eV, real part and imaginary part are zero. The imaginary part is entirely positive. The real part is negative from 0.5 eV to 5 eV. The curves meet starting at 5 eV. The maximum of each (real part and imaginary part) is located at 0 eV.

3.3.2. Optical functions

We determine the different optical functions such as: refractive index $n(\omega)$, extinction coefficient $k(\omega)$, reflectivity $R(\omega)$, absorption coefficient $\alpha(\omega)$ and optical conductivity $\sigma(\omega)$. They are presented by the respective figures 10, 11, 12 et 13.

The complex refractive index predicts photon behavior with respect to the medium during propagation [16, 19]. The real part is the real refractive index n(ω) and the imaginary part, the extinction coefficient k(ω). If n(ω) is high, the light is slow to propagate, it can be deflected. When k(ω) is nonzero, the light is absorbed by the medium. The wave will then weaken more and more during propagation. If k(ω) is zero and n(ω) is positive, the medium is transparent. The real refractive index n(ω) of $NaSrAt_3$ is presented in figure 10.

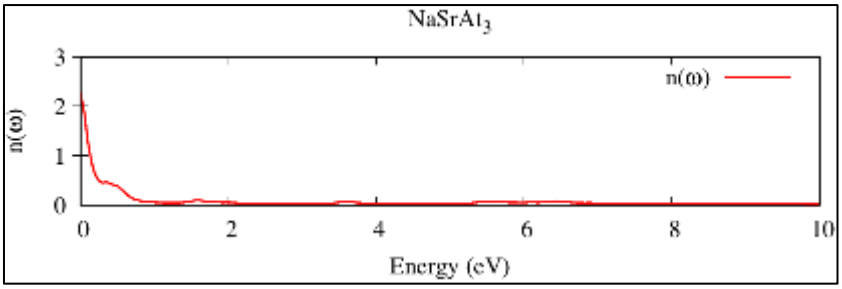

Figure 10 Refractive index for $NaSrAt_3$

It is positive. It includes two parts: from 0 to 2 eV and then from 2 eV to 10 eV. From 0 to 2 eV, the refractive index is positive. It is greater than 1 from 0 to 0.25 eV. Which means that from 0 to 0.25 eV, light passing through $NaSrAt_3$ is likely to be slow to propagate and be deflected in both IR and visible. From 2 eV to 10 eV, the real refractive index n(ω) is practically zero. The main peak is 2.27 to 0.05 eV. Its static value n(0) is 1.705.

Figure 11 presents the extinction coefficient of $NaSrAt_3$. K(ω) characterizes the attenuation of light energy when it passes through a material. The larger the value of K(ω), the higher the interaction between light and matter. This causes a great attenuation of the light wave. On the graph of K(ω), two parts appear: from 0 to 4 eV and from 4 eV to 10 eV. From 4 eV to 10 eV, K(ω) is zero, it is positive from 0 to 4 eV. The main peak is 9.4 at 0.25 eV. K(ω) has a high value between 0 eV and 1 eV, so there is a strong interaction between radiation and material. The light beam is therefore attenuated more strongly. There is absorption of light by the material of 0 eV and 4 eV because K(ω) is non-zero. The intensity of the light then weakens during its propagation in the material.

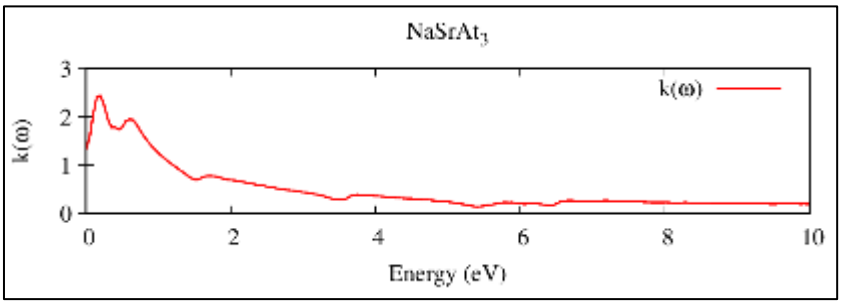

Figure 11 Extinction coefficient for NaSrAt3

Optical reflectivity describes the ability of a material to reflect received light. It compares the intensity of the reflected wave to that of the incident wave. Figure 12 shows the optical reflectivity R(ω) of the perovskite $NaSrAt_3$. The reflectivity reaches its maximum in the energy range 0 to 0.5 eV. From 0 eV to 10 eV, R(ω) increases and reaches 0.9. This increase approximately keeps even if the energy increases. The static reflectivity R(0) of $NaSrAt_3$ is 0.25. This value is above that of $NaSrBr_3$ and $NaSrI_3$ calculated by Yapi et al [17].

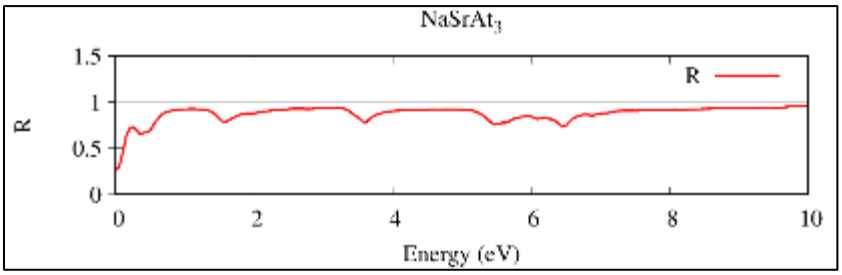

Figure 12 Reflexivity for $NaSrAt_3$

The absorption coefficient α(ω) describes the regression of the intensity of the incident wave passing through a material. The material strongly absorbs light if α(ω) is high. The transmission is then low; there is then a reflection. Furthermore, the material exhibits high transparency if α(ω) is low. α(ω) also explains the type of material. The

absorption coefficient α(ω) of $NaSrAt_3$ is shown in figure 13. According to the graph, the material absorbs from 0 eV up to 2 eV. From 2 eV to 10 eV, absorption is zero. There is therefore absorption by the material in both the visible and IR.

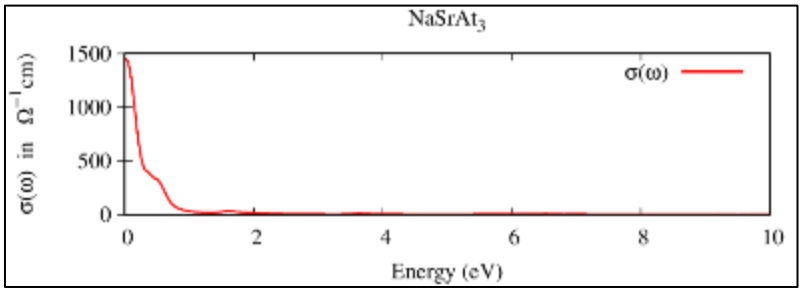

Figure 13 Absorption coefficient for $NaSrAt_3$

To explain the transport of electrons when matter reacts with light, we use the optical conductivity σ(ω) [20]. It also allows understanding the absorption and polarization of the material for a given optical frequency. Figure 14 presents the optical conductivity σ(ω) obtained for the perovskite material $NaSrAt_3$. The static conductivity σ(0) is 4.085×10^5 cm^{-1}. The optical conductivity σ(ω) is strong from 0 eV to 4 eV and weak from 4 eV to 10 eV. There is therefore light-matter interaction with the material from 0 eV to 4 eV. It is concluded that the transport of electrons takes place in this energy interval

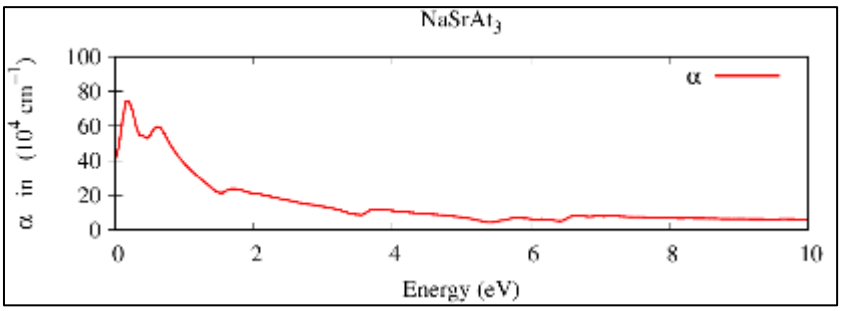

Figure 14 Optical conductivity for NaSrAt3

The electron energy loss function L(ω) reveals the optical energy loss caused by heating or scattering electrons as they pass through a material [19]. Figure 15 shows the energy loss spectrum of the compound $NaSrAt_3$.

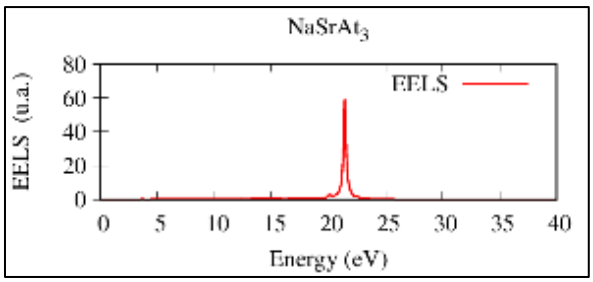

Figure 15 Energy loss function spectrum

Since the studied region is 0 to 10 eV, thus less than 50 eV, the spectrum of L(ω) corresponds to the valence loss spectrum. The graph of L(ω) has a maximum peak at 21.42 eV corresponding to the plasma frequency of the material. It is at this peak that the electrons collectively oscillate under the influence of the electric field of incident light, which is attenuated (screened) by the presence of these electrons.

3.4. Elastic properties

If one wants to study the mechanical and dynamic behavior of the material, it is necessary to explore the elastic properties of this material. For this, independent elastic constants are necessary. For cubic material, these elastic constants are C_{11}, C_{12}, and C_{44} specifically corresponding to directional mechanical responses of the crystal according to directions of forces or stresses applied on these materials [21].

3.4.1. Elastic constants

We present the values of the parameters C_{11}, C_{12}, and C_{44} of $NaSrAt_3$ in table 3. C_{11}, C_{12}, and C_{44} have respectively values 18.73 GPa, 6.58 GPa and 6.58 GPa. C_{11} is greater than C_{12} and C_{44}, so the material has a low pure shear strain resistance compared to unidirectional compressive strength. C_{11}, C_{12}, and C_{44} meet the criteria for mechanical stability of cubic crystals [22,23] :

$$C_{11} > 0 \ ; \quad C_{44} > 0 \ ; \ C_{11} - C_{12} > 0 \ ; \ C_{11} + 2C_{12} > 0$$

Table 1 Elastic constants cubic crystals $NaSrAt_3$

NaSrAt3	
C_{11} (GPa)	18.73
C_{12} (GPa)	6.58
C_{44} (GPa)	6.58
$C_{11} + 2C_{12}$ (GPa)	24.65
$C_{11} - C_{12}$ (GPa)	13.12
$\frac{C_{11}}{C_{12}}$	2.85
$\frac{C_{11}}{C_{44}}$	2.85

3.4.2. Differents mechanical parameters.

Different mechanical parameters can then be determined. Table 4 shows the elastic anisotropy factor A, the bulk modulus B, the Cauchy pressure CP, the Young's modulus E, the Reuss shear modulus (Gr), the Voigt shear modulus (GV), the shear modulus (G), the Poisson coefficient (σ), the Kleinman parameter (ζ), the Pugh ratio (B/G), the Wave Modulus PW, shear constant Cs, Lamé constants (λ and μ), compressibility (β) and the melting temperature Tm.

The compressibility module B is such that $C_{12} < B < C_{11}$, the material $NaSrAt_3$ is therefore stable [22,23]. The anisotropy factor A equals 1.05, a value close to 1 indicating that the material is isotropic. A material is rigid if the Young's modulus (Y) has a high value and slightly rigid if Y is low. We have obtained a value of Y of 0.25 GPa. This shows that the NaSrAt3 material is very non-rigid. The Pugh ratio B/G is 1.67. It is therefore small only 1.75. According to the Pugh criterion [24], the material is fragile. The Poisson coefficient σ characterizes the bond strengths [25]. The value of σ is 0.25. Or a value of σ of 0.25 means an ionic material [25] but also fragile. The quantification of internal stress i.e. the relative ease of bending the bond versus stretching the bond is shown by the Kleinman parameter ζ [26]. ζ is 0.49, there is neither a pure bending of the bond nor a pure stretching of the bond. The hardness shows whether the material is elastic or plastic. The obtained hardness value is 0.10 GPa, a low hardness. The PW wave module measures the ability of a material to resist compression and elongation in the direction of mechanical wave propagation. If PW is high, the material is rigid and additional force will be required for its deformation [27, 28]. We obtained PW values of 13.35 GPa. We obtain a high melting temperature of 664.75 K. $NaSrAt_3$ can be exposed to heat below 664.75 K.

Table 2 Calculated other mechanical parameters for cubic $NaSrX_3$ perovskites

Parameters	**Symbol**	**$NaSrAt_3$**
Elastic constants	C_{11} (GPa)	18.73
	C_{12} (GPa)	6.58
	C_{44} (GPa)	6.58
Anisotropy factor	A	1.054
Voigt bulk moduli	B_V	8.21
Voigt shear moduli	Gv (GPa)	6.38
Reuss shear moduli	Gr (GPa)	6.37
Shear modulus	G (GPa)	6.37
Bulk modulus	B (GPa)	10.63
Cauchy pressure	C_P (GPa)	0.00
Young's modulus	Y (GPa)	0.25
Shear constant	C_S (GPa)	6.07
Poisson's ratio	σ	0.25
Kleinman parameter	ζ(GPa)	0.49
Pugh's ratio	$\frac{B}{G}$	1.67
Hardness	H_v	0.10
Compressibility	β	0,09
Isostatic modulus of elasticity	K	1.00
Isothermal compressibility	X_T (GPa^{-1})	0.99
P-Wave modulus	P_W(GPa)	13.35
Lamé constant	λ (GPa)	0.60
Lamé constant	μ (GPa)	0.60
Melting Temperature	T_m ± 300 (K)	664.75

4. Conclusion

In this study, we determined the structural, electronic, optical and elastic properties of the perovskite material $NaSrAt_3$ by the DFT method using the GGA approximation. We obtained as a lattice parameter a value of 5.15 Å. The gap energy is 0.762 eV and indirect on the Γ-R path. $NaSrAt_3$ is therefore semiconducting and almost conducting. The valence band is characterized by the 1s -At state and the conduction band by the 4p-Na, 2s-Sr and 4p-Sr states. The charge density shows a probable bond between atoms Na and At and atoms Sr and At. Regarding the optical properties, from 0 to 0.25 eV, the light passing through the material is likely to be slower to propagate and to deviate both in IR and in visible. There is a strong interaction between the radiation and the material in this energy range but also an absorption of light by the material. From 2 eV to 10 eV, the real refractive index n(ω) is practically zero. The optical conductivity σ(ω) is strong from 0 eV to 4 eV and weak from 4 eV to 10 eV. Electron transport therefore occurs from 0 eV to 4 eV. As for the elastic properties, the elastic constants found verify well the criteria of mechanical stability. NaSrAt3 has a high fragility but stable however. The anisotropy factor being 1.05, $NaSrAt_3$ exhibits an isotropic character and low hardness. It is very flexible according to the Pugh report. It is likely to be ionic and has neither a pure bending of the bond nor a pure stretching of the bond. The resulting melting temperature is rather high. This study confirms that $NaSrAt_3$ has very good electronic, optoelectronic and elastic and optical properties. It can be used in photovoltaic cells and other electronic devices.

Compliance with ethical standards

Acknowledgments

We would like to thank the Physics Department at Jean Lorougnon Guédé University (UJLoG) in Daloa (Daloa, Côte d'Ivoire) and Fundamental and Applied Physics Laboratory (LPFA) at Nangui Abrogoua University (Abidjan, Ivory Coast) for the collaboration in this study. Their two teams contributed a lot in the realization of this work.

Disclosure of conflict of interest

No conflict of interest to be disclosed.

References

[1] John F. Geisz, Ryan M. France, Kevin L. Schulte et Myles A. Steiner, « Six-junction III–V solar cells with 47.1% conversion efficiency under 143 Suns concentration », Nature Energy, vol. 5, no 4, avril 2020, p. 326–335 (ISSN 2058-7546, DOI 10.1038/s41560-020-0598-5, lire en ligne [archive], consulté le 19 avril 2020).

[2] Abdoulwahab ADAINE. Digital optimization of very high efficiency solar cells based on InGaN [Thesis]. Lorraine, France: Lorraine University . 2018.

[3] Martin A. Green, Keith Emery, Yoshihiro Hishikawa, Wilhelm Warta, and Ewan D. Dunlop. Solar cell efficiency tables (version 48). Progress in Photovoltaics: Research and Applications, 24(7) :905–913, July 2016. 1, 2, 14, 15, 16, 17, 89, 90, 110, 111

[4] Manon SPALLA. Intrinsic stability of perovskite solar cells: impact of the formulation of the active layer and the transport layers of loads [Thesis]. Grenoble, France: Grenoble Alpes University. 2019.

[5] P Giannozzi, O Andreussi, T Brumme, O. Bunau, M. Buongiorno Nardelli, M. Calandra, R Car, C Cavazzoni, D Ceresoli, M Cococcioni, N Colonna, I Carnimeo, A Dal Corso, S de Gironcoli, P Delugas, R A DiStasio Jr, A Ferretti, A Floris, G Fratesi, G Fugallo, R Gebauer, U Gerstmann, F Giustino, T Gorni, J Jia, M Kawamura, H-Y Ko, A Kokalj, E Küçükbenli, M Lazzeri, M Marsili, N Marzari, F Mauri, N L Nguyen; H-V Nguyen, A Otero-de-la-Roza, L Paulatto, S Poncé, D Rocca, R Sabatini, B Santra, M Schlipf, A P Seitsonen, A Smogunov, I Timrov, T Thonhauser, P Umari, N Vast, X Wu and S Baroni (2017). "Advancd capabilities for materials modelling with Quantum ESPRESSO".

[6] P Giannozzi, S Baroni, N Bonini, M Calandra, R Car, C Cavazzoni, D Ceresoli, G L Chiarotti, M Cococcioni, I Dabo, A Dal Corso, S Fabris, G Fratesi, S de Gironcoli, R Gebauer, U Gerstmann, C Gougoussis, A Kokalj, M Lazzeri, L Martin-Samos, N Marzari, F Mauri, R Mazzarello, S Paolini, A Pasquarello, L Paulatto, C Sbraccia, S Scandolo, G Sclauzero, A P Seitsonen, A Smogunov, P Umari, and R M Wentzcovitch. QUANTUM ESPRESSO: a modular and open-source software project for quantum simulations of materials. Journal of Physics: Condensed Matter. (2009), 21(39), p. 395502.

[7] A M Rappe, K M Rabe, E Kaxiras and J D Joannopoulos. Optimized pseudopotentials. Phys. Rev. B 44, (1991), 13175.

[8] J P Perdew, K Burke, K and M G Ernzerhof. Generalized Gradient Approximation Made Simple. Phys Rev Lett. 77(1996)3865 and Phys Rev Lett. 78(1997)1396.

[9] [A D Becke. Density-functional exchange-energy approximation with correct asymptotic behavior. In: Physical Review A, (1988), 38(6), p. 3098–3100.

[10] J P Perdew, K Burke and M Ernzerhof. Generalized Gradient Approximation Made Simple. [Phys. Rev. Lett. 77, 3865 (1996)]. In: Physical Review Letters, (1997), 78(7), p. 1396-1396.

[11] Md Tanvir Hossain, F-T Zahr, R A-A Dhroobo, Md M Hasan, Md R Al Amin, F M A Sieam, S Swargo, S T Disha, R Islam. First-principles insights into the structural, mechanical, electronic, optical, and thermophysical properties of $XSrBr_3$(X = Na, Ga, and Tl) perovskites: Implications for optoelectronic applications. Materials Science in Semiconductor Processing 182 (2024) 10869.

[12] Md Tanvir Hossain, Tasmi A, Jahirul I, Md Al-A B Shuvo a, K Hossain, Md A Hossain. Investigation of structural, mechanical, electronic, optical, and thermodynamic properties of AXI_3(A = Li, Na; X = Ca, Sr, and Ba) halide perovskites for emerging energy technologies: A DFT study; Materials Science in Semiconductor Processing. Volume 188. 2025. 109235.

[13] Robinson Outerovitch. Study of Effective Electronic Interactions in Strongly Correlated Solids. [Thesis]. Paris, France : Paris-Sacley University. 2022.

[14] H J Monkhorst and J D Pack. Special Points for Brillouin-Zone Integrations. Physical Review B. (1976). Vol 13. pp 5188-5192.

[15] Maskar Elhoussaine. Ab-initio study of the Magnetic, Optical, and Thermoelectric Transport Properties of materials: Case of the $Ga_{1-x}(4f)_xN$, SnO, et Bi_2CrMO_6 (M=Zn, Ni) [Thesis]. Rabat, Morocco: Mohammed V University. 2022.

[16] Dian Dwiriani, M Z Efendi, R Aritonang, T U Lestari. Band gap energy characteristics in materials. Journal of frontier research in science and engineering. 3(2)(2025).

[17] Mona Hermann Charly YAPI, Guy Müller Banquet OKRA, Mélèdje C. Désiré, Niaré Adama, Kré N'Guessan N Raymond. Study of the structural, electronic, optical, and elastic properties of $NaSrX_3$ (X = Br and I) perovskites using Density Functional Theory (DFT) with GGA formalism. World Journal of Advanced Research and Reviews (WJARR), 2025, 28(01), 160-174.

[18] A.H. Reshak, Z.A. Alahmed, S. Azam, Electronic structure, electronic charge density and optical properties analyses of $Rb_2Al_2B_2O_7$ compound: DFT calculation, Int. J. Electrochem. Sci. 9 (2014) 975–989, https://doi.org/10.1016/S1452-3981(23)07771-4.

[19] J Islam, K Hossain. First-principles simulations to investigate effect of hydrostatic pressure on structural, mechanical, electronic, and optical properties of the $AgCdCl_3$ perovskite. Emergent Mater 6 (2023) 1763–1777. https://doi.org/ 10.1007/s42247-023-00565-1.

[20] A Darvishzadeh, N Alharbi, A Mosavi, N E Gorji. Modeling the strain impact on refractive index and optical transmission rate. Phys B Condens. Matter 543 (2018) 14–17. https://doi.org/10.1016/j.physb.2018.05.001.

[21] J Lelièvre. New lead-free materials based on bismuth: towards lead-like compounds (A,A')(B)O_3 et (A,A')(BB')O_3. University doctoral thesis. Specialty: Ceramic materials and surface treatments. University of Limoges, France. 2017. 210 p.

[22] M Houari, B Bouadjemi, M Matougui, S Haid, T Lantri, Z Aziz, S Bentata and B Bouhafs. Optoelectronic properties of germanium iodide perovskites $AGeI_3$ (A= K, Rb and Cs): 1st principles investigations. In : Springer Nature. (2019). Vol. 51. No. 7. p 1–14.

[23] M Houari, B Bouadjemi, S Haid, M Matougui, T Lantri and Z Aziz. Semiconductor behavior of halide perovskites $AGeX_3$ (A = K, Rb, Cs; X = F, Cl Br): first-principles calculations. Indian J Phys. (2019). Vol. 97. pp 1-13.

[24] S F Pugh. Relations between the elastic moduli and the plastic properties of polycrystalline pure metals. The London Edinburgh and Dublin Philosophical Magazine and Journal of Science. (1954). Vol 45. No 367. pp 823–843.

[25] A Meziani. Study of the structural, electronic, elastic, and optical properties of CsCdF3 and $KZnF_3$ fluoro-perovskite compounds. University doctoral thesis, Specialization: Condensed Matter Physics. Mokhtar Badj University, Algeria. 2012. 95 p.

[26] B Kleinman, M Karplus; Phys Rev. B 3 (1971) 24.

[27] S Chibani, O Arbouche, M Zemouli, Y Benallou, K Amara, N Chami, M Ameri, M E Keurti. First-principles investigation of structural, mechanical, electronic, and thermoelectric properties of Half-Heusler compounds RuVX (X=As, P, and Sb). Comput Condens Matter 16. (2018) e00312. https://doi.org/10.1016/j.

[28] Mavko G, Mukerji T, and Dvorkin J. (1998) The Rock Physics Handbook: Tools for Seismic Analysis in Porous Media. Cambridge University Press, 208-210.